Results in Physics 19 (2020) 103332

Contents lists available at ScienceDirect

Results in Physics

journal homepage: www.elsevier.com/locate/rinp

Peculiarities of electronic structure and composition in ultrasound milled silicon nanowires

E.V. Parinova[a,*], A.K. Pisliaruk[a], A. Schleusener[b], D.A. Koyuda[a], R.G. Chumakov[c], A.M. Lebedev[c], R. Ovsyannikov[d], A. Makarova[e], D. Smirnov[f], V. Sivakov[b], S.Yu. Turishchev[a]

[a] Voronezh State University, Universitetskaya pl. 1, 394018 Voronezh, Russia
[b] Leibniz Institute of Photonic Technology, Albert Einstein Str. 9, 07745 Jena, Germany
[c] National Research Center "Kurchatov Institute", Akademika Kurchatova pl. 1, 123182 Moscow, Russia
[d] Helmholtz-Zentrum Berlin, Albert Einstein Str. 15, 12489 Berlin, Germany
[e] Free University of Berlin, Arnimallee 22, 14195 Berlin, Germany
[f] Dresden University of Technology, Zellescher Weg 18, 01062 Dresden, Germany

ARTICLE INFO

Keywords:
Silicon
Nanoparticles
Suboxide
Ultrasoft X-ray spectroscopy
Synchrotron radiation
Electronic structure and composition

ABSTRACT

The combined X-ray absorption and emission spectroscopy approach was applied for the detailed electronic structure and composition studies of silicon nanoparticles produced by the ultrasound milling of heavily and lowly doped Si nanowires formed by metal-assisted wet chemical etching. The ultrasoft X-ray emission spectroscopy and synchrotron based X-ray absorption near edges structure spectroscopy techniques were utilize to study the valence and conduction bands electronic structure together with developed surface phase composition qualitative analysis. Our achieved results based on the implemented surface sensitive techniques strongly suggest that nanoparticles under studies show a significant presence of the silicon suboxides depending on the prenature of initial Si wafers. The controlled variation of the Si nanoparticles surface composition and electronic structure, including band gap engineering, can open a new prospective for a wide range Si-based nanostructures application including the integration of such structures with organic or biological systems.

X-ray emission and absorption spectroscopy are ultimate techniques allowing not only the studies of surface chemical composition, but also provide the extended information on the electronic structure and the local surrounding of the given atoms [1–5] in the studied material. On the other hand, ultrasoft X-ray techniques allow the surface sensitive studies in nanometer range [6–8] which makes such techniques even more attractive for direct experimental determination of nanosized structures characteristics [9–12]. As it is well-known, Si nanostructures play the ultimate role in the modern micro- and nanoelectronics [13]. Si nanowires [14] formed by a simple and convenient metal assisted wet-chemical etching technique [14,15] is one of a best example of the well-conceived Si technology step that allows to control and combine a number of functional properties of such nanostructures. In addition, such nanowires can be used for the formation of Si nanoparticles with a developed surface, which allows their implementation in medicine or biomaterial related fields [16,17]. The application of the ultrasoft X-ray emission (USXES) and X-ray absorption near edge structure spectroscopy (XANES) techniques for the precision studies of the local Si atoms surrounding, electronic structure and composition of the powders formed from the different doping level Si nanowires is a main focus in present paper.

Silicon nanoparticles (SiNPs) were produced from wet-chemically etched heavily (10^{-19} cm^{-3}, HD) and lowly (10^{-15} cm^{-3}, LD) n-type phosphorous doped Si nanowires (SiNWs) followed by their fragmentation in non-polar organic solvent (*iso*-propanol) by using an ultrasound bath (37 kHz, 90 W) for 4 h [18,19]. Sivakov et al. previously have been discussed the morphology and structure difference in lowly and heavily doped SiNWs, where the heavily doped SiNWs show more rougher and porous or nanostructured morphology in comparison to lowly doped SiNWs [20,21]. Finally, the solvent was evaporated using rotary evaporator system and produced solid nanoparticles (LD-pwd and HD-pwd) were permanently stored in flask under argon atmosphere prior to X-ray spectroscopy experiments. SiNPs were in contact with the environment for about 15 min (partial surface oxidation) during the preparation of the sample for X-ray spectroscopic studies.

USXES Si $L_{2,3}$ spectra provide information on the local partial density of occupied electronic states distribution in the valence band and were obtained with the use of laboratory RSM-500 high vacuum

* Corresponding author.
E-mail address: parinova@phys.vsu.ru (E.V. Parinova).

https://doi.org/10.1016/j.rinp.2020.103332
Received 30 June 2020; Received in revised form 11 August 2020; Accepted 14 August 2020
Available online 17 August 2020

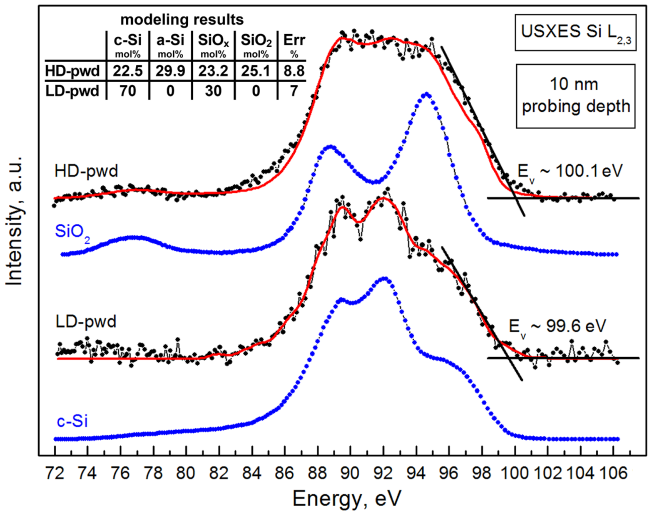

Fig. 1. USXES Si $L_{2,3}$ experimental spectra (black curves) and simulated (red curves) of HD-pwd and LD-pwd with E_v position approximation. c-Si and SiO_2 reference spectra are given for comparison (blue curves). Inset (table): estimated composition at 10 nm probing depth.

spectrometer. The obtained spectra were subjected to computer simulation for the semi-quantitative estimation of surface composition [1,2,10]. Probing depth was 10 nm [2,8,10] and energy resolution below 0.3 eV. XANES Si $L_{2,3}$ spectra give an insight into distribution of local partial density of free electronic states in the conduction band and were obtained at two high intensity synchrotron facilities: Kurchatov at NRC "Kurchatov Institute" and HZB BESSY II storage rings. Ultra-high vacuum end-stations Nano-PES and RGL-PES were used. XANES Si $L_{2,3}$ probing depth was about 5 nm [7] and energy resolution below 0.1 eV [9,22].

The obtained USXES Si $L_{2,3}$ spectra are presented in the Fig. 1. The difference between the valence band electronic state density distributions in the SiNPs under study is clearly visible. LD-pwd USXES spectrum is closer to the known reference of c-Si [1–3,10]. In comparison, HD-pwd has noticeably smeared fine structure spectrum with the clearly observed increasing in density of states (see ranges ~89 eV or 93 eV and higher). It's a specific indication to the presence of disordering up to amorphization [23–24] of initial c-Si surface. The fitting table (Fig. 1 inset) gives us a semi-quantitative estimation of the LD- and HD-pwd composition at 10 nm probing depth.

The presence of a-Si phase according to fine structure and modeling results (see a-Si reference spectrum used in [23–24]) indicates that Si atoms closest neighbors and their coordination deviations in the inner volume of the particles cause smearing and a general increase in the density of states distribution. After simulation the presence of SiO_x phase (Fig. 1 inset) in HD-pwd as a more appropriative result of highly developed surface of SiNPs (and initial wires). The SiO_x reference spectrum is a sum of $SiO_{0.47}$ and $SiO_{1.3}$ phases in USXES Si $L_{2,3}$ spectra [25]. The valence band top position E_v estimated in Fig. 1 and gives a difference of 0.5 eV between HD and LD powders (100.1 eV and 99.6 eV, respectively) that can be caused by sufficiently higher content of suboxide and interatomic disordering in HD-pwd sample.

XANES Si $L_{2,3}$-edge spectra for LD- and HD-pwd are given together with the references of c-Si and SiO_2 in Fig. 2. In general, the fine structure distribution of given spectra is in good correlation with observed USXES results. Features related to c-Si in 101–102 eV and 102.5–103.5 eV ranges of HD-pwd XANES spectrum are not sharp resolved. This observation indicates the presence of silicon with the certain degree of disorder in HD-pwd NPs [9,10,22]. The dip at ~ 100 eV in LD-pwd spectrum can be caused by interaction of silicon particles with synchrotron radiation that was previously observed for SiNWs [9]. Nevertheless, 100–103.5 eV fine structure confirms the presence of

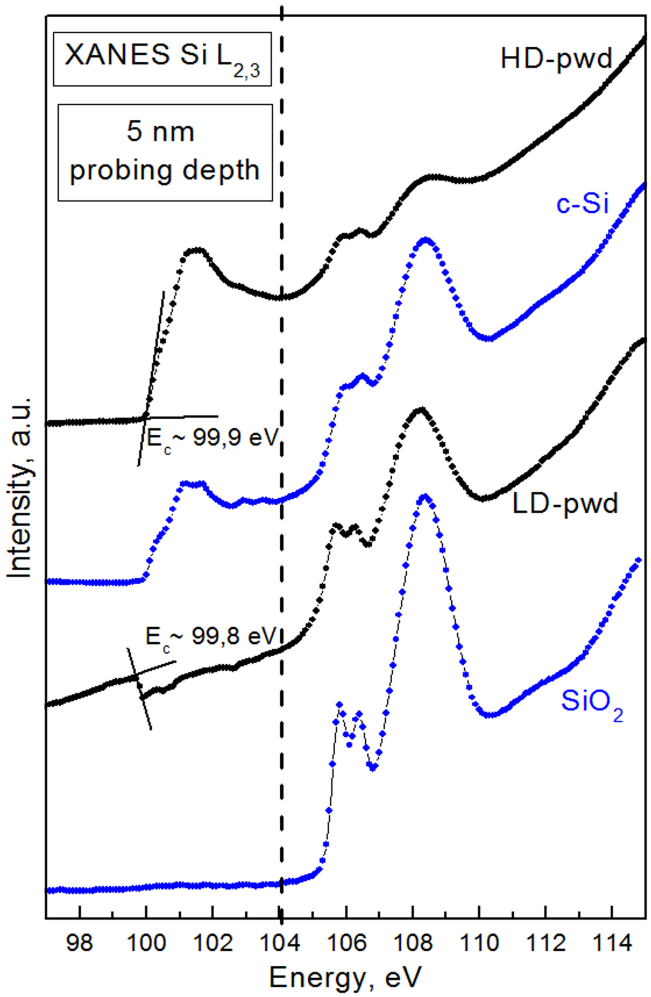

Fig. 2. XANES Si $L_{2,3}$ synchrotron spectra of HD-pwd and LD-pwd with E_c position approximation. References spectra of c-Si and SiO_2 are given (blue curves) for comparison.

ordered Si atoms within probing depth (~5 nm) also in LD-pwd NPs surface. The conduction band bottom position E_c values 99.9 eV and 99.8 eV for HD-pwd and LD-pwd, respectively (see Fig. 2) are comparable with the bulk Si conduction band values.

Spectral features higher than 104 eV correspond to the presence of Si-oxides [4,9,22,23] in both samples. The observed fine structure is closer to SiO_2 that is reasonable with respect to the probing depth. The trace of SiO_x interlayer observed by USXES can be supported by the wider 108 eV peak for HD-pwd and smooth rise for LD-pwd in XANES spectra intensity after 103.5 eV [4]. Differences in relative intensities distribution of the Si-oxide spectral part can be explained by the different oxidation degree that is in a good agreement with USXES results and can be caused by more developed surface of HD-pwd NPs [20,21].

In summary, combined XANES and USXES Si $L_{2,3}$ analysis of lowly and heavily doped SiNPs allows to underline changes in band gap width, probably caused by composition and atomic ordering changes in studied nanoparticles. The developed surface of the nanoparticles with significant amount of the silicon suboxides, with controlled variation of the composition and electronic structure, including gap engineering, has a great prospective for a wide range of applications, including the integration with organic or biological systems.

CRediT authorship contribution statement

E.V. Parinova: Conceptualization, Methodology, Investigation,

Writing - original draft, Writing - review & editing, Supervision, Project administration. **A.K. Pisliaruk:** Methodology, Validation, Formal analysis, Investigation. **A. Schleusener:** Methodology, Resources, Investigation. **D.A. Koyuda:** Methodology, Resources, Investigation, Validation. **R.G. Chumakov:** Methodology, Validation, Investigation, Writing - review & editing. **A.M. Lebedev:** Methodology, Validation, Investigation, Writing - review & editing. **R. Ovsyannikov:** Methodology, Validation, Investigation. **A. Makarova:** Methodology, Validation, Investigation. **D. Smirnov:** Methodology, Validation, Investigation. **V. Sivakov:** Conceptualization, Methodology, Investigation, Writing - original draft, Writing - review & editing, Supervision, Project administration, Funding acquisition. **S.Yu. Turishchev:** Conceptualization, Methodology, Investigation, Writing - original draft, Writing - review & editing, Supervision, Project administration, Funding acquisition.

Declaration of Competing Interest

The authors declare that they have no known competing financial interests or personal relationships that could have appeared to influence the work reported in this paper.

Acknowledgements

The study was supported by Russian Science Foundation (Project 19-72-20180). ST additionally acknowledges the Ministry of Science and Higher Education of the Russian Federation under State Task for Higher Education Organizations in Science for 2020-2022 (Project FZGU-2020-0036) in part of USXES experiments data evaluation. V.S. acknowledges the financial support for nanoparticles formation and characterization by the German Research Foundation (DFG, Grant No. SI1893/18-1). The results were partially obtained on the equipment Joint Facilities Center of Voronezh State University. The authors thank the Helmholtz-Zentrum Berlin für Materialien und Energie for support within the bilateral Russian-German Laboratory program.

References

[1] Zatsepin DA, Kaschieva S, Zier M, et al. Soft X-ray emission spectroscopy of low-dimensional SiO2/Si interfaces after Si+ ion implantation and ion beam mixing. Phys Status Solidi A 2010;207(3):743. https://doi.org/10.1002/pssa.200925469.

[2] Domashevskaya EP, Peshkov YA, Terekhov VA, et al. Phase composition of the buried silicon interlayers in the amorphous multilayer nanostructures $[(Co_{45}Fe_{45}Zr_{10})/a\text{-}Si{:}H]_{41}$ and $[(Co_{45}Fe_{45}Zr_{10})_{35}(Al_2O_3)_{65}/a\text{-}Si{:}H]_{41}$. Surf Interface Anal 2018;50(12–13):1265. https://doi.org/10.1002/sia.6515.

[3] Kurmaev EZ, Galakhov VR, Shamin SN, et al. Local structure of porous silicon studied by means of X-ray emission spectroscopy. Appl Phys A Mater Sci Process 1997;65:183. https://doi.org/10.1007/s003390050563.

[4] Barranco A, Yubero F, Espinos JP, et al. Electronic state characterization of SiOx thin films prepared by evaporation. J Appl Phys 2005;97(11):113714https://doi.org/10.1063/1.1927278.

[5] van Buuren T, Dinh LN, Chase LL, et al. Changes in the Electronic Properties of Si Nanocrystals as a Function of Particle Size. Phys Rev Lett 1998;80(17):3803. https://doi.org/10.1103/PhysRevLett.80.3803.

[6] Erbil A, Cargill III GS, Frahm R, et al. Total-electron-yield current measurements for near-surface extended X-ray absorption fine structure. Phys. Rev. B. 1988;37:2450. https://doi.org/10.1103/PhysRevB.37.2450.

[7] Kasrai M, Lennard WN, Brunner RW, et al. Sampling depth of total electron and fluorescence measurements in Si L- and K-edge absorption spectroscopy. Appl Surf Sci 1996;99:303. https://doi.org/10.1016/0169-4332(96)00454-0.

[8] Zimina AV, Shulakov AS, Eisebitt S, et al. Depth-resolved soft X-ray emission spectroscopy of Si-based materials. Surf Rev Lett 2002;09(01):461. https://doi.org/10.1142/S0218625X02002464.

[9] Turishchev SYu, Parinova EV, Pisliaruk AK, et al. Surface deep profile synchrotron studies of mechanically modified top-down silicon nanowires array using ultrasoft X-ray absorption near edge structure spectroscopy. Sci Rep 2019;9:8066. https://doi.org/10.1038/s41598-019-44555-y.

[10] Turishchev SYu, Terekhov VA, Kashkarov VM, et al. Investigation of the electron energy structure and phase composition of porous silicon with different porosity. J Electron Spectrosc Relat Phenom 2006;156–158:445. https://doi.org/10.1016/j.elspec.2006.11.037.

[11] Zatsepin AF, Buntov EA, Zatsepin DA, et al. Energy band gaps and excited states in Si QD/SiOx/RyOz (R = Si, Al, Zr) suboxide superlattices. J Phys: Condens Matter 2019;31:41. https://doi.org/10.1088/1361-648X/ab30d6.

[12] Sylenko PM, Shlapak AM, Petrovska SS, et al. Direct nitridation synthesis and characterization of Si_3N_4 nanofibers. Res Chem Intermed 2015;41:10037. https://doi.org/10.1007/s11164-015-2011-8.

[13] Hiller D, Duffy R, Strehle S, et al. Advances in silicon-nanoelectronics, nanostructures and high-efficiency Si-photovoltaics. Phys Status Solidi A 2020;217:2000023. https://doi.org/10.1002/pssa.202000023.

[14] Lo Faro MJ, Leonardi AA, D'Andrea C, et al. Low cost synthesis of silicon nanowires for photonic applications. J Mater Sci: Mater Electron 2020;31:34. https://doi.org/10.1007/s10854-019-00672-y.

[15] Sandu G, Osses JA, Luciano M, et al. Kinked silicon nanowires: superstructures by metal-assisted chemical etching. Nano Lett 2019;19(11):7681. https://doi.org/10.1021/acs.nanolett.9b02568.

[16] Gongalsky M, Gvindzhiliia G, Tamarov K, et al. Radiofrequency hyperthermia of cancer cells enhanced by silicic acid ions released during the biodegradation of porous silicon nanowires. ACS Omega 2019;4(6):10662. https://doi.org/10.1021/acsomega.9b01030.

[17] Song B, He Y. Fluorescent silicon nanomaterials: from synthesis to functionalization and application. Nanotoday 2019;26:149. https://doi.org/10.1016/j.nantod.2019.03.005.

[18] Tolstik E, Osminkina LA, Matthäus C, et al. Studies of silicon nanoparticles uptake and biodegradation in cancer cells by raman spectroscopy. Nanomedicine 2016;12(7):1931. https://doi.org/10.1016/j.nano.2016.04.004.

[19] Shevchenko SN, Burkhardt M, Sheval EV, et al. Antimicrobial effect of biocompatible silicon nanoparticles activated using therapeutic ultrasound. Langmuir 2017;33(10):2603. https://doi.org/10.1021/acs.langmuir.6b04303.

[20] Sivakov VA, Voigt F, Berger A, et al. Roughness of silicon nanowire sidewalls and room temperature photoluminescence. Phys Rev B 2010;82:125446https://doi.org/10.1103/PhysRevB.82.125446.

[21] Turishchev SYu, Terekhov VA, Nesterov DN, et al. Atomic and electronic structure peculiarities of silicon wires formed on substrates with varied resistivity according to ultrasoft X-ray emission spectroscopy. Tech Phys Lett 2015;41:344. https://doi.org/10.1134/S106378501504015X.

[22] Turishchev SYu, Terekhov VA, Parinova EV, et al. Surface modification and oxidation of Si wafers after low energy plasma treatment in hydrogen, helium and argon. Mater Sci Semicond Process 2013;16:1377. https://doi.org/10.1016/j.mssp.2013.04.020.

[23] Terekhov VA, Parinova EV, Domashevskaya EP, et al. Peculiarities of the electronic structure and phase composition of amorphous (SiO2)x(a-Si: H)x–1 composite films according to X-ray spectroscopy data. Tech Phys Lett 2015;41:1010. https://doi.org/10.1134/S1063785015100296.

[24] Domashevskaya EP, Terekhov VA, Turishchev SYu, et al. Atomic and electronic structure of amorphous and nanocrystalline layers of semi-insulating silicon produced by chemical-vapor deposition at low pressures. J Synch Invest 2015;9:1228. https://doi.org/10.1134/S1027451015060257.

[25] Wiech G, Feldhutter HO, Simunek A. Electronic structure of amorphous SiOx: H alloy films studied by X-ray emission spectroscopy: Si K, Si L, and O K emission bands. Phys Rev B 1993;47:6981. https://doi.org/10.1103/PhysRevB.47.6981.